Obat: Jurnal Riset Ilmu Farmasi dan Kesehatan
Volume. 3 Nomor. 1 Tahun 2025
e-ISSN : 3031-0148, dan p-ISSN : 3031-013X, Hal. 60-74
DOI: https://doi.org/10.61132/obat.v3i1.900
Available online at: https://journal.arikesi.or.id/index.php/OBAT

CT scan assessment of Olfactory Fossa in Kirkuk adult population prior to sinus surgery

Karim Mahmood Hussein
Radiology lecturer at college of medicine, University of Kirkuk.
E-mail: *karimazaw@uokirkuk.edu.iq*

Abstract. *The fovea ethmoidalis and the lateral lamella of the cribriform plate of the ethmoid bone are the parts of the skull base that are most vulnerable to iatrogenic problems during functional endoscopic sinus surgery. The vertical height of the cribriform plate's lateral lamella, which is divided into three groups based on Keros types. According to the Keros, The likelihood of iatrogenic injury and issues increases with the cribriform plate's lateral lamella height.*

Keywords: *CT scan, Olfactory fossa, Sinus surgery*

Aim of the study:

The aim of this study is to assess the discrepancies in the ethmoid roof elevation (the depth of the olfactory fossa) amongst the adult Kirkuk population using multi-detector computed tomography.

Patients and methods:

160 persons who were referred for a CT scan to evaluate their paranasal sinuses participated in the study. Participants in this study were not allowed to have any pathological abnormalities affecting the ethmoid roof. According to the Keros classification, which was split into three groups (Keros I from 1 to 3 mm, and from 4 to 7 mm considered Keros II, while Keros III should be from 8 mm and more), the vertical height of the lateral lamella of the cribriform plate was measured using the coronal portion of a CT image.

Results:

The patients' average age was 35.25 ±14.16 years. The range of the left lateral lamella height is 2.1 to 10.0 mm, and the range of the right lateral lamella height is 2.0 to 9.9 mm. Of these, 43.75% had Keros type I, 55% had Keros type II, and 1.25% had Keros type III.

Conclusion:

Keros type II was present in the majority (about 55%) of the adult population in that was studied while Keros type I was (about 43.75%). However, just (about 1.25%) of the adults population in the sample had Keros type III.

Introduction

Received: November 22, 2024; Revised: November 07, 2024; Accepted: Desember 23, 2024;
Online Available: Desember 27, 2024

One important bone component integrated into the anterior skull base is the ethmoid cross. This structure is composed of a horizontal limb called the cribriform plate, which forms the ethmoid roof and separates the nasal recess of the nasal cavity below from the olfactory fossa above. The

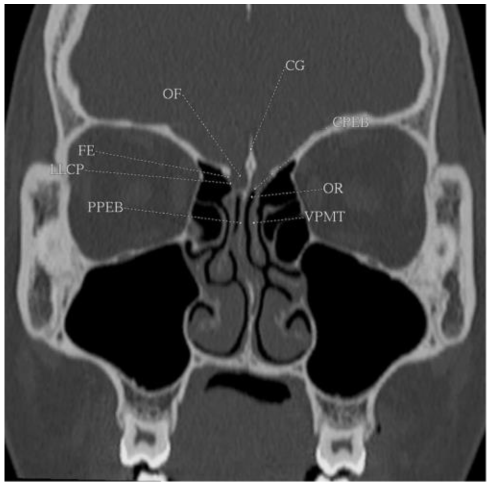

valuable olfactory nerve and bulb are located in the olfactory fossa, which is the most infero-medial part of the anterior cranial fossa. The perpendicular plate under the horizontal limb and the crista galli above it make up the longitudinal limb. One component of the anterior bone that contributes to the development of the ceiling of the ethmoid bony labyrinth is the fovea ethmoidalis (FE). It divides the anterior cerebral fossa from the ethmoidal air cells. Additionally, FE articulates medially with the lateral [(1)] (Fig. 1). The skinniest bone in the whole base of the skull is the LLCP (2,3). The areas of the skull base that are most susceptible to iatrogenic complications during functional endoscopic sinus surgery include FE and LLCP. FESS [(2,3,4,5,6,7)] . Fig. 1[(1)]

The anatomical characteristics of the ethmoid roof include the VPMT vertical plate of the middle turbinate, LLCP lateral lamella of the cribriform plate, CG crista galli, OF olfactory fossa, FE fovea ethmoidalis, PPEB perpendicular plate of ethmoid bone, OR olfactory recess, and CPEB cribriform plate of ethmoid bone.

Keros (1962) labeled deviations in the parallel level of the cribriform plate of the ethmoid bone. According to his explanation of three likely levels in his German book, he distributed the olfactory fossa's deepness into three sets. Later then, this has been identified as Keros classification. The cribriform plate's lateral lamella length determines the keros classification. The lateral margin of the cribriform is joined by this thin, primarily vertical bone plate. The later bony structure, which is actually the most medial portion of the orbital plate of the frontal bone that forms the orbital roof, is the bony ceiling of the ethmoid air cells (the ethmoid labyrinth). [(8)].

Keros's original description is that the ethmoid roof is nearly in the same plane as the cribriform plate, the lateral lamella is small, and the olfactory fossa is 1-3 mm deep in Keros I (26.3% of the population). The lateral lamella is longer and the olfactory fossa is 4–7 mm deep in Keros II (73.3% of the population). The olfactory fossa in Keros III, which comprises 0.5% of the population, is 8–16 mm deep, and the ethmoid roof is situated considerably above the cribriform plate. [(8)].

However, the Keros classification did not identify dimensions between 3 and 4 mm or between 7 and 8 mm. Measurements between 0 and less than 4 mm were referred to as Type 1 Keros in a number of investigations. Type 2 Keros were defined as measurements of 4 mm or more but less than 8 mm, and Type 3 Keros were defined as measurements of 8 mm or more. The olfactory fossa will get deeper and smaller as the LLCP height increases. Additionally, the ethmoid roof will be lower. [(9)]. Therefore, the risk of iatrogenic damage increases with LLCP height (10). In essence, keros type III leaves the thin LLCP vulnerable to possible harm from surgery, trauma, tumor erosion, and CSF erosion. Endoscopic sinus surgery (ESS) is recommended for a variety of conditions and procedures, such as mucocele, sellar and parasellar tumors, optic nerve decompression, nasal polyposis, and other intracranial lesions, in addition to treating chronic rhinosinusitis that does not improve with therapy. [(10)].

The widespread adoption of ESS is not without its issues. These might be classified as either minor or major issues. Minor issues occur in between 1.1 to 20.8% of patients involving functional endoscopic sinus surgery.Ostial stenosis, numbness of the teeth or lips, infection, crusting, development of synechiae, bleeding, and illness recurrence are among them. [(11)] .

0–1.5% of these operations result in serious complications. These include cerebral injury (damage to the brain or major blood arteries), cerebrospinal fluid leak, and ocular injury (herniation of orbital fat, extraocular muscle injury, ocular motility dysfunction, optic nerve injury, and peri-orbital hemorrhage or peri-orbital emphysema). [(11,12)] .

Most of the primary issues have something to do with the ethmoid bone. The following anatomical alterations have been reported in patients with chronic rhinosinusitis: 30% have conchae bullosa, 24% have paradoxical middle turbinate, 21% have septal deviation, 15% have agger nasi cells, 7% have Haller cells, [(13)].

A thorough evaluation of chronic rhinosinusitis and variations in paranasal anatomy are necessary for the efficacy of FESS. With frequently less invasive treatments, FESS can dramatically improve recurrent or persistent sinusitis problems if these variants are identified. [(14)].

By themselves, anatomic abnormalities of the paranasal sinuses do not constitute disease states;

rather, they degrade existing restricted drainage routes and generate severe blockage. These anatomic variations are common, may affect surgical safety, and must be explicitly looked for during the preoperative assessment (14).

The preferred diagnostic technique for assessing the ostiomeatal complex at the moment is MDCT, which can show both soft tissues and bone. MDCT serves as a preoperative map to help the surgeon navigate the area's difficult and diverse anatomy as well as a diagnostic tool to detect anatomical abnormalities and mucosal pathology (13, 15).

Aim of the study

The aim of this study was to assessed olfactory fossa depth among adult population and associated nasal and para nasal anatomical variants which is a relevant area in endoscopic sinus surgery injury or complications, by using multi detectors computed tomography . We classify the measurements using the Keros classification after using the vertical height of the lateral lamella of the cribriform plate (LLCP).

Patients and methods

The patients' data were collected from Radiology department in the Azadi teaching hospital in a period From the January 2019 to the March 2020 .The patients referred from the ENT outpatient clinic their ages were from 18 years and above. The survey study was to the olfactory fossa depth, Then analyzed these measurements with the age, gender and associated nasal and para nasal anatomical variants .

Inclusion criteria

This study was conducted on 160 adult Iraqi patients who were referred for multi-detector computed tomography imaging in order to evaluate the para-nasal sinuses for potential inflammatory or malignant alterations. This study was conducted in complete compliance with the rules. All of the patients were over the age of eighteen, with half of them being men and the other half being women.

Exclusion criteria

Patients under the age of eighteen and those with lesions that destroyed or concealed the olfactory fossa or olfactory recess were excluded. To avoid any potential impact on the skull structure, we only included adult Iraqis in our routine sample and did not include members of other racial or ethnic groups.

Multi Detectors Computed Tomography (MDCT) Examination:

We told all patients about the examination and instructed them to be not moved during the examination.64 slice multi detectors CT machine (Siemens, system SOMATOM Definition AS made in Germany) used in patients examination.

In supine position and put the patient head symmetrically in the head rest at first takes lateral scout view and planning for axial imaging, then get coronal reconstruction images. Without angulation (Tilt 0) axial imaging were gotten.

200 mAs, 120 kV, 1 mm portion width, huge field of view (FOV), and 0.8 pitch were the parameters of the procedure.The acquired images were rebuilt at 0.65 mm using a high resolution bone filter (70s sharp) and soft tissue.Using a workstation (Siemens, system SOMATOM Definition AS manufactured in Germany) to manipulate the modified images' data Multi-planner reformation (MPR) creates several distinct planes.

Line A is a horizontal line that connects the inferior orbital foramina's upper edge. A perpendicular line (Line B) drawn between (Line A) connects the lateral lamella of the cribriform plate in the ethmoid bone (LLCP) with the fovea ethmoidalis (medial aspect of the orbital plate of the frontal bone). Another line, Line C, is drawn vertically between Line A and the ethmoid bone's cribriform plate on the lateral aspect.

The height of the cribriform plate was shown by Line C, and the height of the medial ethmoid roof was shown by Line B.(Fig.2).

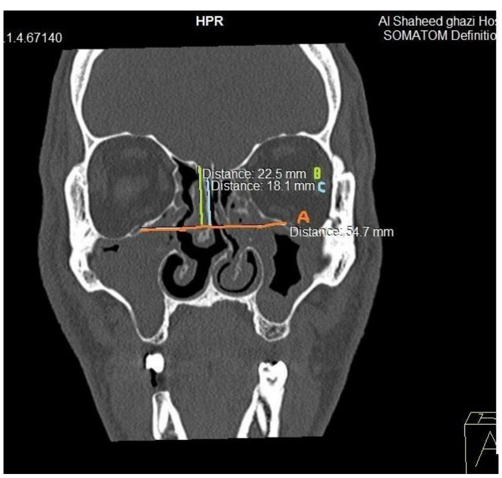

Figure (2)

The measurements are shown using lines A, B, and C. (4.4 mm) = 22.5–18.1 is the right (h). On the right, type (II). Asymmetry and somewhat varying levels of vertical angulation may be seen in both LLCP.

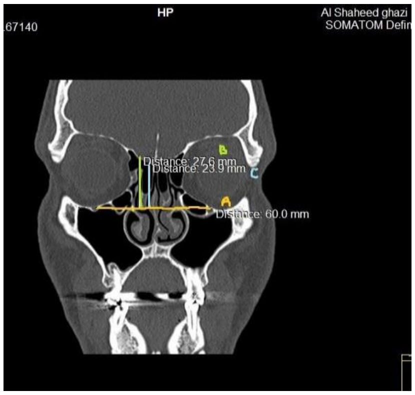

Figure (3) Keros Type (I) olfactory fossae on the RT side(h)=27.6-23.9= (3,7mm).

The depth of the olfactory fossa representing the height of the ethmoid roof "h" that obtained from the length of the Line B "b" minus the length of the line C "c" so " h=b-c " in millimeters, this resulting the vertical height of lateral lamella of the cribriform plate of the ethmoid bone (LLCP) and show different angulations according to the anterior skull base configuration. Even by sub-millimeters measurement can be obtained by modern available multi detectors CT (MDCT) software. So type I Keros representing measurement below the 4mm And Keros type II showed measurements between 4 mm and less than 8mm while measurements from 8 mm and above considered Keros type III. In the classification of the original Keros types , the measurements more than three millimeter and below than four millimeter are not described also the measurements that represent morethan seven millimeter and less than eight millimeter.

Statistical analysis

by quantitatively analyzing gathered data measures using the statistical package for the social sciences (SPSS). The mean and standard deviation of these statistics were described. The differences based on gender type were also compared between the right and left sides.These metrics were categorized according to Keros kinds.
The p-values for the student t-test and the paired t-test were computed and compared between the means of the right and left sides, respectively. Additionally, the right and left sides are correlated using the r:person coefficient. We compared males and females based on the Keros types classification, and the p-value for the Monte Carlo test was ($p < 0.05$), which indicates statistical

significance.

Results

160 adult Iraqi patients were selected for multi-detector computed tomography (MDCT) scans.Of the 80 patients, half were men, while the other half were women. The patients ranged in age from 18 to 85 years old, with a mean age of 35.25 ±14.16 years. The men' mean age was 34.8 ± 14.10 years, while the females' mean age was 35.69 ±14.21 years.

The LLCP cribriform plate's lateral lamella (also known as the average height of the ethmoid roof or "h") had an average vertical height of 4.2 ±1.18 mm. The average "h" for the right side was 4.25 ± 1.16 mm, whereas the average for the left side was 4.15± 1.15 mm.

.The average difference between the left- and right-sided "h," however, was ($p = 0.10$). It was discovered that the average "h" on the left side was lower.

When the "h" of the right and left sides were matched for each One, 12 cases (7.5%) showed asymmetry, or a height difference of more than 1 mm between the right and left sides. Lower left-sided ethmoid roofs were found in seven cases (4.375%), whereas lower right-sided ethmoid roofs were seen in five cases (3.125%). The distribution of lateral lamella cribriform plate depth in symmetry and asymmetry groups is displayed in Table 1.

Table 2 displays the patient distributions based on the Keros categorization types. Based on the lateral lamella of cribriform plate height (LLCP), 140 (43.75%) sides have Keros I, 176 (55%) sides have Keros II, and 4 (1.25%) sides have Keros III. Nearly all (58.12%) of the females' olfactory fossa were of Keros type II, whereas about 41.87% were of Keros type I. There was no Keros type III of olfactory fossa height in the female subjects. Type I and Type II represent 71 and 85 olfactory fossae in males, correspondingly, whereas the remaining 4 were of Keros type III.

The most prevalent in both males and females was type II. Only males were found to have Type III. The average LLCP height for Keros I individuals was 3.22 ±0.53 mm, for Keros II instances it was 4.85 ±0.66 mm, and for Keros III cases it was 9.50 ± 0.68 mm. Table 3 showed the outcomes for both parties.

Table(1) lateral lamella of cribriform plate height distribution insymmetry and asymmetry groups .

Sex			
– – – – – – – – – –			
Male		female	overall
Right> Left with > 1 mm	3	2	5
Left> Right with> 1 mm	4	3	7
Total asymmetry (right or left)	7	5	12
Symmetry	73	75	148
Overall (symmetry+ asymmetry)	80	80	160

Fig(4): Distribution and percentage values of LLCP depth in symmetry

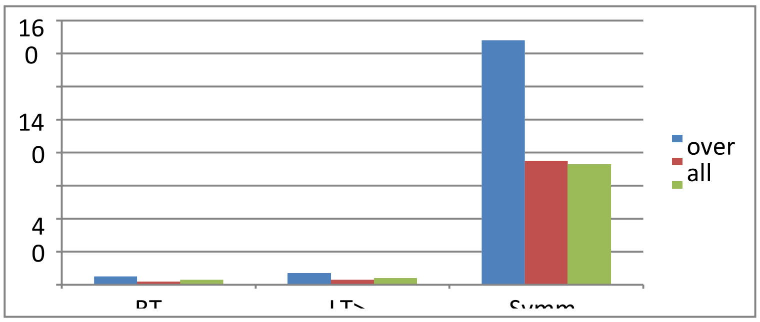

and asymmetry groups.

Table 2	Relation between the Keros Types and the sex.		
Sex			
– – – – – – – – – – – – – – – – – –			
Male		female	
		overall	
Keros Type			
Type I (1–3.9)	72	68	140
Type II (4–7.9)	84	92	176
Type III (8– more)	4	0	4
p	0.2*		

p: p value for Monte Carlo test to compare between the males andthe females according to the types.

* Statistically significant at $p \leq 0.05$.

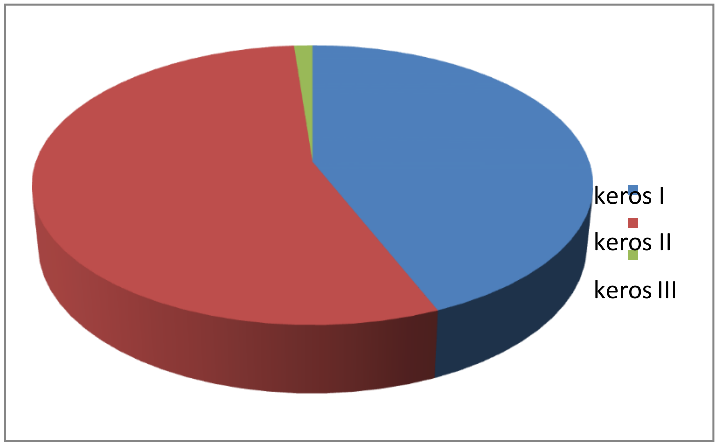

Fig (5) distribution cases according to keros type .

Table 3 Keros Types and LLCP height in relation to one other on the right and left

Keros Type			
	Type I	Type II	Type III
Right			
Mean ± SD	3.23±0.51	4.84±0.71	9.2±0.98
Left			
Mean ± SD	3.21±0.55	4.87±0.60	9.8±0.28
Overall			
Mean±SD	3.22±0.53	4.85 ±0.66	9.50 ±0.68

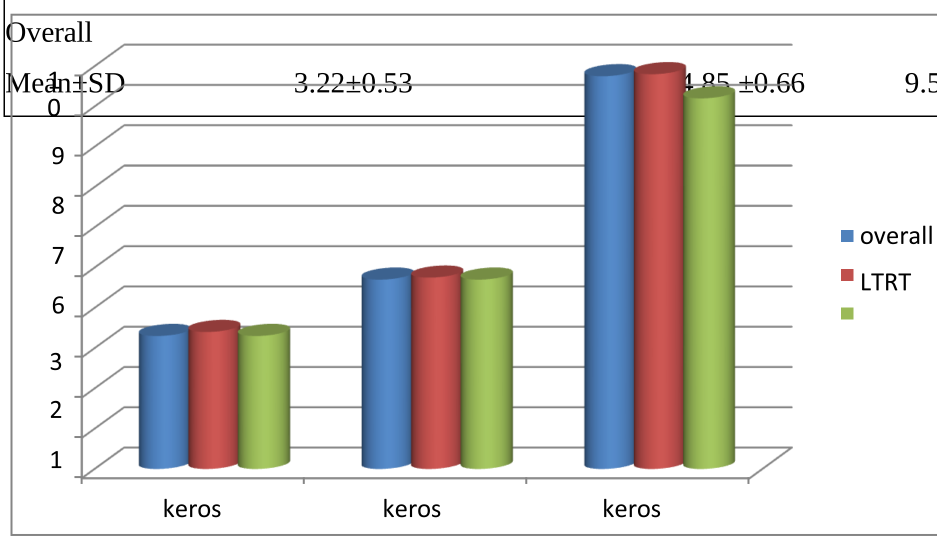

Fig (6) Keros Types and height on the right and left sides, as well as overall

Discussion

FE and LLCP are both operating on the ethmoid air cells' bony roof. On the ethmoid air cell roof, the FE forms a robust lateral side. The thinnest bony plate at the base of the skull is thought to be the LLCP. Its width was measured between 0.05 and 0.2 mm. The most susceptible region for endoscopic surgery problems, intracranial perforations, and iatrogenic injuries is the LLCP. It is the weak medial side of the bone roof of the ethmoid air cell. (31).

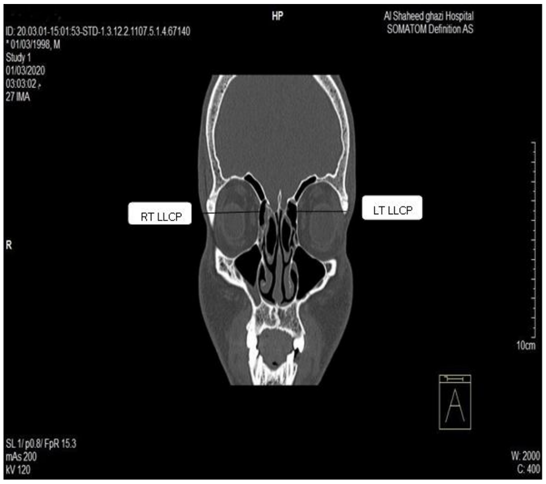

Fig. (7) Asymmetry in the shape of the each olfactory fossa. On theRight side the fossa is wider than Left side and slightly more in the vertical height.

The vertical angulation of LLCP is seen in different degrees (Fig. 7). The LLCP-FE link's placement indicated the olfactory fossa configuration from the intracranial side and the olfactory recess depth and ethmoidal roof height from the nasal side. Since length and LLCP are sides of a right angle triangle, their total vertical angulation determines the depth of the olfactory fossa. LLCP is the right angle triangle's hypotenuse. The olfactory fossa narrows and deepens as the vertical depth of the LLCP increases, while the ethmoid roof lowers and seems to hang. So this will. In our investigation The left ethmoid roof can theoretically be more susceptible to iatrogenic[1,3,33] .

In our study, Type I was found in 43.75% of the population, compared to 26.3% in the original Keros types classification (8). 73.3% of patients had the Keros II olfactory fossa, compared to 55% in our study. Compared to 0.5% of the population, 1.25% of the participants in this study had the Keros type III olfactory fossa described.

The original Keros types classification does not define measurements between 7 and 8 mm, or larger than 3 mm and less than 4 mm. On the other hand, in our study, we categorized measures larger than 3 and smaller than 4 mm as Keros type I and measurements between 7 and 8 mm as Keros type II

Table 4 compares the incidence of the different types of Keros in different studies among populations of different races. The proportions of different studies that looked into different ethnic and demographic groupings differed. In terms of the metrics that were initially unclear, the number of patients analyzed, the measurement technique, and even the standardization of the Keros categories (greater than 3 mm and less than 4 mm as well as between the 7 mm and 8 mm) are some examples of how these differences can be seen.

Table 4 Keros types classification among different studies

Author	Country	Keros I (%)	Keros II (%)	Keros III (%)
Original Keros (6)	Germany	26.3	73.3	0.5
This study	Iraq	43.75	55	1.25
Elwany et al. (31)	Egypt	42.5	56.8	0.7
Kaplanoglu et al.(29)	turkey	13.4	76.1	10.5
Solares et al. (5)	USA	83.0	15.0	2.0
Souza et al. (2)	Brazil	26.3	73.3	0.5
Paber et al. (4)	Philippine	81.8	17.7	0.5
Bista et al. (36)	Nepal	86.0	12.0	2.0

For this study, we employed multi-detector computed tomography in the dimensions. The measurements in this work are based on the anatomical location of the infra-orbital nerves. Throughout the procedure and endoscopic sinus surgery ESS, this reference point is crucial. We could help the doctors figure out how deep the ethmoid roof is. The Additional Research (4, 31, 34, 35). Furthermore, the anatomy, which varies even between the two sides of the same patient, was assessed using the same anatomical markers that were used to illustrate the map in the coronal photographs. These multi-detector coronal CT slices are essential for assessing trouble spots and for planning endoscopic sinus surgery (ESS). The most frequent adverse consequence of endoscopic sinus surgery is ethmoid bone problems. [36]

The assessment of the ethmoid roof, which is essential for avoiding or lessening the issues associated with functional endoscopic sinus surgery, has been the subject of numerous studies. [36, 37]. Anatomical variations, particularly in the base of the skull, should be precisely characterized and reported in reports in order to prevent or minimize any issues. [2, 3].

Table 5 shows the anatomical variations seen in our investigation.

Table 5. the Distribution and the proportion values of anatomic discrepancies according to the gender

	Male %	**female** n(80) %	**total n(80)** n(160) %
Concha bullosa	26 (32.5%)	30(37.5%)	56(35%)
Intra-lamellar air Cell	9(11.25%)	3(3.75%)	12(7.5%)
Paradoxal middle concha	3(3.75%)	2(2.5%)	5(3.12%)
Pneumatized agger nasi	------	2(2.5%)	2(1.25%)
Haller cell	3(3.75%)	-----	3(1.87%)
Nasal septum deviation	25(31.25%)	10(12.5%)	35(21.8)
Spur formation	5(6.25%)	2(2.5%)	7(4.3%)
Pneumatized cresta galli	2(2.5%)	------	2(1.25%)

Limitations of the study

Patients sampled in this work were not large in number, and the selections were in a nonspecific decade among the adult Iraqi population.So we have different decades and also the individuals younger than 18 years old not involved in this study.

Conclusion

1. In our work we studied Iraqi adult population, showed Keros II (55%) and followed by keros type I (43.75%). While Keros III is noted in only 1.25% of the studied adult Iraqi community.
2. In this study, males were marginally more likely than females to have a low or deep ethmoid roof.
3. Height of the LLCP constitutionally different and must be well evaluated during the preoperative assessment of the sinus CT.

4. The use of preoperative CT measures may enhance the evaluation and best surgical management of the anatomical differences of the skull base.

References

Al-Abri, R., Bhargava, D., Al-Bassam, W., et al. (2014). Clinically significant anatomical variants of the paranasal sinuses. *Oman Medical Journal*, 29(2), 110–113.

Alkire, B. C., & Bhattacharyya, N. (2010). An assessment of sinonasal anatomic variants potentially associated with recurrent acute rhinosinusitis. *Laryngoscope*, 120, 631–634.

Altimimi, M. L., & Ali, A. K. (2024). Examining the impact and complexity of sinusitis complications in the Iraqi population and their treatment. *European Journal of Modern Medicine and Practice*, 4(4), 315–325.

Beale, T. J., Madani, G., & Morley, S. J. (2009). Imaging of the paranasal sinuses and nasal cavity: Normal anatomy and clinically relevant anatomical variants. *Seminars in Ultrasound, CT, and MRI*, 30, 2–16.

Bhargava, D., Bhargava, K., Al-Abri, A., et al. (2011). Non-allergic rhinitis: Prevalence, clinical profile and knowledge gaps in literature. *Oman Medical Journal*, 26(6), 416–420.

Chaitanya, C. S., et al. (2015). Computed tomographic evaluation of diseases of paranasal sinuses. *International Journal of Recent Scientific Research*, 6(7), 5081–5086.

Dessi, P., Castro, F.,

Duvoisin, B., Landry, M., Chapuis, L., Krayenbuhl, M., Schnyder, P. (1991). Low-dose CT and inflammatory disease of the paranasal sinuses. *Neuroradiology*, 33, 403–406.

Elwany, S., Medanni, A., Eid, M., Aly, A., El-Daly, A., & Ammar, S. R. (2010). Radiological observations on the olfactory fossa and ethmoid roof. *Journal of Laryngology and Otology*, 124, 1251–1256.

Faiq, S. Y., & Dewachi, Z. (2023). Three-dimensional evaluation of maxillary sinus volume, skeletal and dentoalveolar maxillary anterior region, in unilateral palatally impacted maxillary canine (Cross-sectional study). *Journal of Orthodontic Science*, 12(1), 75.

Fatterpekar, G., Delman, B., & Som, P. (2008). Imaging the paranasal sinuses: Where we are and where we are going. *Anatomical Record*, 291(11), 1564–1572.

Gotwald, T. F., Zinreich, S. J., Corl, F., & Fishman, E. K. (2001). Three-dimensional volumetric display of the nasal ostiomeatal channels and paranasal sinuses. *AJR American Journal of Roentgenology*, 176(1), 241–245.

Kainz, J., & Stammberger, H. (1988). The roof of the anterior ethmoid: A locus minoris resistentiae in the skull base. *Laryngologie, Rhinologie, Otologie*, 67, 142–149.

Kaplanoglu, H., Kaplanoglu, V., Dilli, A., Toprak, U., & Hekimoglu, B. (2013). An analysis of the anatomic variations of the paranasal sinuses and ethmoid roof using computed tomography. *Eurasian Journal of Medicine*, 45, 115–125.

Keast, A., Yelavich, S., Dawes, P., & Lyons, B. (2008). Anatomical variations of the paranasal sinuses in Polynesian and New Zealand European computerized tomography scans. *Otolaryngology-Head and Neck Surgery*, 139, 216–221.

Keros, P. (1962). On the practical value of differences in the level of the lamina cribrosa of the ethmoid. *Z Laryngologie, Rhinologie, Otologie Ihre Grenzgeb*, 41, 808–813.

Keros, P. (1965). On the practical importance of differences in the level of the cribriform plate of the ethmoid. *Laryngologie, Otologie, Rhinologie*, 41, 808–813.

Luong, A., & Marple, B. F. (2006). Sinus surgery: Indications and techniques. *Clinical Reviews in Allergy & Immunology*, 30, 217–222.

Luong, A., & Marple, B. F. (2006). Sinus surgery: Indications and techniques. *Clinical Reviews in Allergy & Immunology*, 30, 217–222.

Mafee, M. F. (1991). Endoscopic sinus surgery: Role of the radiologist. *AJNR American Journal of Neuroradiology*, 12(5), 855–860.

McMains, K. C. (2008). Safety in endoscopic sinus surgery. *Current Opinion in Otolaryngology & Head and Neck Surgery*, 16, 247–251.

Miller, J. C. (2009). Imaging for sinusitis. *Radiology Rounds: A Newsletter for Referring Physicians*, Massachusetts General Hospital Department of Radiology, 7(8).

Momeni, A. K., Roberts, C. C., & Chew, F. S. (2007). Imaging of chronic and exotic sinonasal disease: Review. *AJR American Journal of Roentgenology*, 189, S35–S45.

Paber, J. A. L., Cabato, M. S. D., Villarta, R. L., & Hernandez, J. G. (2008). Radiographic analysis of the ethmoid roof based on KEROS classification among Filipinos. *Philippine Journal of Otolaryngology Head and Neck Surgery*, 23(1), 15–19.

Shama, S. A., & Montaser, M. (2015). Variations of the height of the ethmoid roof among Egyptian adult population: MDCT study. *Egyptian Journal of Radiology and Nuclear Medicine*, 46(4), 929–936.

Shpilberg, K. A., Daniel, S. C., & Doshi, A. H. (2015). CT of anatomic variants of the paranasal sinuses and nasal cavity: Poor correlation with radiologically significant rhinosinusitis but importance in surgical planning. *American Journal of Roentgenology*, 204(6), 1255–1260.

Solares, C. A., Lee, W. T., Batra, P. S., & Citardi, M. J. (2008). Lateral lamella of the cribriform plate: Software-enabled computed tomographic analysis and its clinical relevance in skull base surgery. *Archives of Otolaryngology-Head & Neck Surgery*, 134(3), 285–289.

Souza, S. A., Souza, M. M. A., Idagawa, M., Wolosker, A. M. B., & Ajzen, S. A. (2008). Computed tomography assessment of the ethmoid roof: A relevant region at risk in endoscopic sinus surgery. *Radiologia Brasileira*, 41(3), 143–147.

Spector, S. L., Berstein, I. L., Li, J. T., et al. (1998). Joint task force on practice parameters, joint council of allergy, asthma and immunology. Parameters for the diagnosis and management of sinusitis. *Journal of Allergy and Clinical Immunology*, 102(6, part 2), S107–S144.

Stammberger, H. (1993). Endoscopic anatomy of lateral wall and ethmoidal sinuses. In H. Stammberger & M. Hawke (Eds.), *Essentials of functional endoscopic sinus surgery* (pp. 13–42). Mosby-Year Book.

Terrier, F., Weber, W., Ruefenacht, D., & Porcellini, B. (1995). Anatomy of the ethmoid: CT, endoscopic and macroscopic. *AJR, American Journal of Roentgenology*, 144, 493–500.

Ulualp, S. O. (2008). Complications of endoscopic sinus surgery: Appropriate management of complications. *Current Opinion in Otolaryngology & Head and Neck Surgery*, 16, 252–259.

Ulualp, S. O. (2008). Complications of endoscopic sinus surgery: Appropriate management of complications. *Current Opinion in Otolaryngology & Head and Neck Surgery*, 16, 252–259.

Yousem, D. M. (1993). Imaging of sinonasal inflammatory disease. *Radiology*, 188(2), 303–314.

Zinreich, J. S. (1998). Functional anatomy and computed tomography imaging of the paranasal sinuses. *The American Journal of the Medical Sciences*, 316(1), 2–12.

Zinreich, S. (1997). Rhinosinusitis: Radiologic diagnosis. *Otolaryngology-Head and Neck Surgery*, 117(3), 27–34.